

Optimization of Operating Conditions of a Household Up-draft Biomass Gasification Stove

Shuanghui Deng, Xuebin Wang, Houzhang Tan,* Yan Li, Zhongfa Hu, and Ben Niu

Experiments were carried out with a household up-draft biomass gasification stove to investigate effects of the air distribution method on the performance of the stove. The temperature distribution along the gasifier, the producer gas composition, the stove power, and the thermal efficiency were investigated. Results showed that in the temperature distribution along the gasifier height, the highest temperature was at the bottom oxidation layer of the gasifier, in the range of 950 to 1050 °C. With increasing air quantity through the burner, the time required to boil the water first decreased and then increased, whereas the stove power and thermal efficiency increased and then decreased. The best stove performance was obtained at an optimum air distribution ratio of 0.333 between burner and gasifier air ($0.794 \times 10^{-3} \text{ m}^3/\text{s}\cdot\text{kg}$). When the burner air increased, the flame length above the burner was remarkably reduced and the flame color gradually changed from yellow-red to blue. At the optimum air distribution ratio of 0.333, the flame was blue and stable. The present study provides references for developing a more efficient biomass gasification stove.

Keywords: Biomass; Stove; Air distribution; Gasification stove; Optimization; Efficiency

Contact information: MOE Key Laboratory of Thermo-Fluid Science and Engineering, School of Energy and Power Engineering, Xi'an Jiaotong University, Xi'an 710049, China;

* *Corresponding author:* tanhz@mail.xjtu.edu.cn

INTRODUCTION

Biomass is widely regarded as a potential renewable, carbon-neutral energy source and is especially important in developing countries. Biomass accounts for more than 90% of the total rural energy supplies in underdeveloped countries, and 10% to 15% of the world's primary energy consumption (Qiu *et al.* 1996; Bhattacharya and Salam 2002). Increasing research attention has been focused on biomass use, with concerns of global warming and energy shortage growing. Currently, over two billion people use biomass-derived energy to cook every day (MacCarty *et al.* 2008). Even though the traditional, small-scale stove degrades air quality and is thermally inefficient, biomass is still commonly used in small-scale stoves for household cooking or warming because it is simple and cheap (Panwar 2009).

Many studies have been conducted to characterize small cookstove performance (Ballard-Tremere and Jawurek 1996; McCracken and Smith 1998; Boy *et al.* 2000; Bailis *et al.* 2007; Jetter *et al.* 2012). These studies indicate that the efficiency of biomass utilization for cooking could be enhanced by two to three times and that the efficiency of traditional biomass-fired cooking stoves is in the range of 5% to 20%. However, recent, more advanced types of stoves can be more than 30% efficient (Bhattacharya *et al.* 2002; Yuntanwi *et al.* 2008; Panwar 2010; Li *et al.* 2011; Huangfu *et al.* 2014).

Recent works on biomass stoves have focused primarily on pollutant emissions (Brauer *et al.* 1995; Smith *et al.* 2000; Ezzati and Kammen 2001; Reddy and Venkataraman 2002; Koyuncu and Pinar 2007; Johnson *et al.* 2011). Comparisons of different kinds of stoves indicate that the fan stove and the gasifier stove emit relatively few particulates and greenhouse gases (Smith *et al.* 1993; MacCarty *et al.* 2008). The gasifier stove has the potential for higher-efficiency, lower-emission, small-scale biomass utilization. However, there are many problems with the application of biomass gasifier stoves, including the low gas heat value, poor fuel adaptability, and high tar content.

Many previous studies have focused on the final efficiency and emissions. Research on the reaction process in the stove has been insufficient, although very important for building a theoretical basis for emission control and efficiency improvement in stoves. In the present study, the effect of the air distribution method (including the overall air quantity into the stove system and the ratio of air supplied between the gasifier and burner) on the performance of a household up-draft biomass gasification stove was investigated. The temperature distribution and gas composition along the gasifier were determined, and the gasified gas heat value and thermal efficiency of the stove were calculated.

EXPERIMENTAL

Gasification Stove

The tested gasification stove system is shown in Fig. 1. It consisted of gasifier, air supplying and distribution, burner, gas sampling, and temperature measurement sections. The gasifier was made of a refractory steel tube with an inside diameter of 290 mm and a heating-length of 330 mm. The outside diameter of the gasifier was 385 mm. Along the height of the gasifier, six sampling holes were fixed into one side of the gasifier to measure the gas composition at heights of 50, 125, 200, 275, 350, and 425 mm. On the other side of the gasifier, four K-type thermocouples accurate to within 1 °C were installed to measure the central temperatures at heights of 90, 215, 335, and 455 mm. The distributed air blown into the gasifier or burner could be adjusted using the valves on the branch pipes.

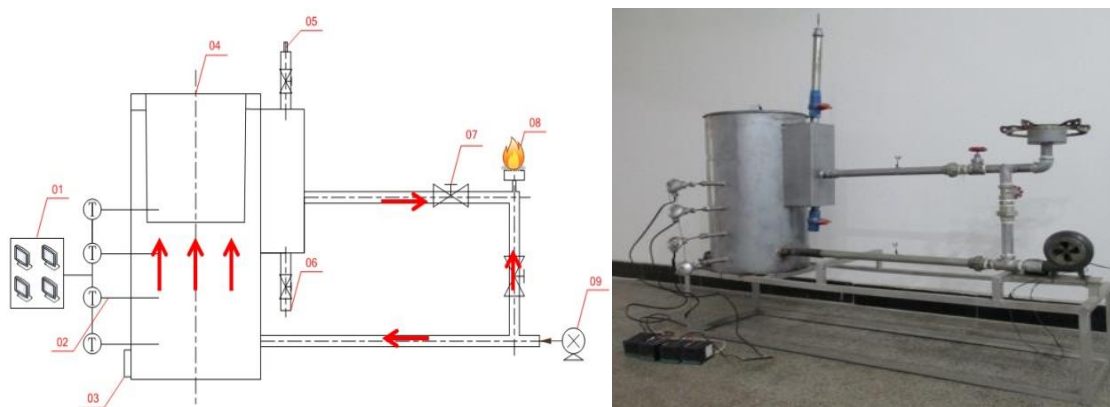


Fig. 1. Experimental gasification stove system: 01 - temperature recorder; 02 - thermocouple; 03 - ash outlet; 04 - gasifier; 05 - gas sampling; 06 - tar collector; 07 - air distribution valve; 08 - gas burner, and 09 - air blower

Fuel Properties

Previous studies (Wang *et al.* 2012, 2014) have shown that the differences between different kinds of agricultural biomass are relatively minor. Straw, the most common crop waste in China, was used in the present investigation. It was acquired from the city of Baoji in western China. The fuel properties are listed in Table 1.

Table 1. Proximate and Ultimate Analyses of Straw Used in Gasification Stove

Fuel	$Q_{net,al}$ (MJ/kg)	Proximate Analysis (wt. %)				Ultimate Analysis (wt. %)					
	$Q_{net,d}$	M_{ad}	A_{ad}	V_{ad}	FC_{ad}	C_{ad}	H_{ad}	N_{ad}	O_{ad}	$S_{t,ad}$	Cl_{ad}
Straw	14.77	3.88	6.01	72.1	18.01	43.92	4.47	0.44	40.98	0.3	0.486

Measurement and Calculation Methods

The entire 8 kg of biomass was loaded into the gasifier in one batch. The gasifier was preheated to the desired temperature through the external heater strip at the bottom until some fuel gas was produced at the top of the gasifier. Next, the top half of gasifier was covered with a lid, and the external heater was closed. The air from the air blower was fed into the gasifier. The test began. The temperature and gas distribution in the gasifier stove reached a steady state after a period of time. The temperature values were obtained by the temperature recorders. During the test, a small amount of tar from the gasifier appeared in the tar collector. The fuel gas was ignited by an open flame on the top of the gas burner. A kettle filled with water was placed above the burner. The producer gas was sampled at the outlet of the gasifier and analyzed using a gas chromatograph-mass spectrometer (GC-MS, GCMS-QP2010 Ultra, Shimadzu, Japan) and a flue gas analyzer (Gasmeter DX-400, Gasmeter Technologies, Finland). The heating value (MJ/m³) of the gasified gas was calculated according to the mole fractions of the constituent gas species. The water temperature was measured by a kerosene thermometer.

The water boiling method (Li *et al.* 2011) was used to determine the output power (kW) and thermal efficiency (%) according to the time from ambient temperature to 95 °C after boiling temperature. The output power of the stove is defined as,

$$P_{stove} = \frac{E_s + E_L}{t_1 - t_2} \quad (1)$$

where P_{stove} is the stove power (kW), E_s is the sensible heat required to raise the water from room temperature to boiling temperature (kJ), E_L is the latent heat (kJ), t_1 is the time when the water temperature was 95 °C after boiling (s), and t_2 is the time when water heating began (s).

The stove thermal efficiency (Li *et al.* 2011) is defined as,

$$\eta_{stove} = \frac{E_s + E_L}{M_{WL} Q_{net}} \times 100 \quad (2)$$

where η_{stove} is the thermal efficiency (%), M_{WL} is the mass of fuel burned (kg), and Q_{net} is the lower heating value of the fuel (kJ/kg).

Gasification efficiency and carbon conversion also describe the performance of the gasifier and are defined as,

$$\eta_{gas} = \frac{\text{Gas heating value (kJ} \cdot \text{m}^{-3}) \times \text{gas production rate (m}^3 \cdot \text{kg}^{-1})}{\text{Heating value of biomass fuel (kJ} \cdot \text{kg}^{-1})} \quad (3)$$

$$\eta_{\text{carbon}} = \frac{12 \times (CV_{CO_2} + CV_{CO} + CV_{CH_4})}{22.4 \times \left(\frac{298}{273}\right) \times C_{\text{carbon}}} \times G_V \quad (4)$$

where CV is the species volume content in the gas produced (%), G_V is the production rate of gasified gas (m^3/kg), and C_{carbon} is the carbon content in the biomass fuel used.

Gas heating value is the lower heating value in this work, and its calculation formula is as follows,

$$Q = 12.64 V_{CO} + 18.79 V_{H_2} + 35.88 V_{CH_4} + 64.35 V_{C_2H_6} + 59.44 V_{C_2H_4} \quad (5)$$

where Q is the gas heating value (MJ/m^3), and V_{CO} , V_{H_2} , V_{CH_4} , $V_{C_2H_6}$, and $V_{C_2H_4}$ (vol%) are the volumes of the respective gas components of the producer gas.

Test Conditions

Two groups of tests were conducted in this study. In the first, all air was supplied to the gasifier and there was no air supplied to the burner. These tests were done to investigate the effect of the air quantity supplied on the gasifier. Under these conditions, the flame on the burner was a diffusion flame. The air quantities into the gasifier tested were 0.265×10^{-3} , 0.529×10^{-3} , 0.794×10^{-3} , and $1.058 \times 10^{-3} \text{ m}^3/\text{s} \cdot \text{kg}$. The unit of air quantity is $\text{m}^3/\text{s} \cdot \text{kg}$, the air quantity per unit mass biomass fuel. In each test, 8 kg of biomass was loaded into the gasifier.

In the second group of tests, the air quantity into the gasifier was held constant at the optimum value from the first group of tests, and the air quantity into the burner was either 0, 1.27×10^{-3} , 2.117×10^{-3} , or $2.717 \times 10^{-3} \text{ m}^3/\text{s}$, corresponding to gasifier-to-burner air ratios of 0, 0.2, 0.333, and 0.428.

RESULTS AND DISCUSSION

Temperature and Gas Distribution in the Gasifier

Layer analysis in the up-draft gasifier

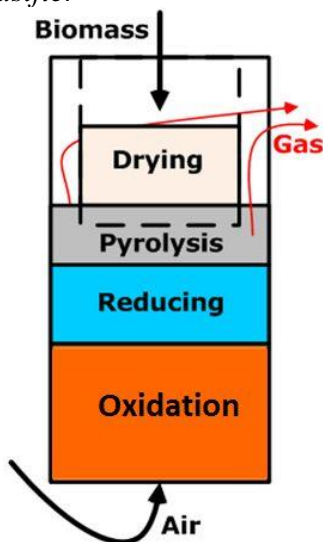
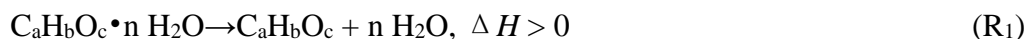


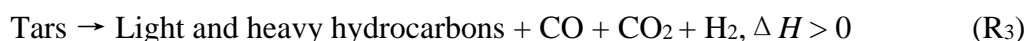
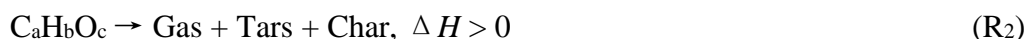
Fig. 2. Layered reaction structure in an up-draft gasifier

The gasification process in an up-draft gasifier can be divided into four layers: drying, pyrolysis, reduction, and oxidation, from top to bottom, as shown in Fig. 2. In the present gasifier, these layers corresponded to heights of 455, 335, 215, and 90 mm, respectively.

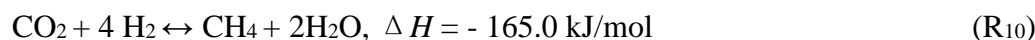
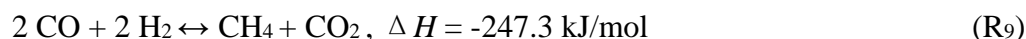
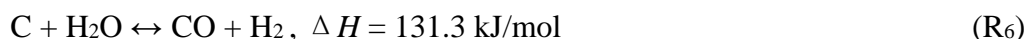
In the drying layer, the water in the biomass was removed in the following reaction,



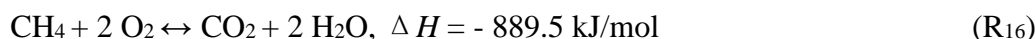
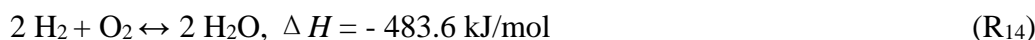
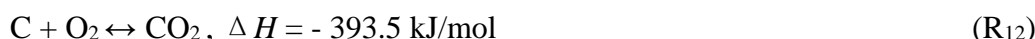
In the pyrolysis layer, the volatiles in the biomass decomposed into gas and tar, producing char as follows,



In the reducing layer, both CO_2 and H_2O can be reduced to CO , H_2 , and CH_4 by char at high temperatures as described by the following reactions,



In the oxidation layer at the bottom of the gasifier, biomass is oxidized in the presence of air as described by the reactions,



The four layers of reaction structure were set up and will be used further in data analysis. Most importantly, the temperature distribution was in a dynamic relation with the tests. Along with the going of reaction in the gasifier, the general temperature increased, ash was produced and stacked at the bottom, consequently, these four reaction layers moved upwards.

Temperature

The temperature distribution along the gasifier height at different times is shown in Fig. 3. Measuring the temperature at different heights is important, especially in building the layered reaction structure model of the gasifier. The results obtained in the experiment can be used to verify the model. In addition, according to the temperature distribution at different heights and the reaction model, the gas distribution at different heights could be obtained. Under these conditions, all air passed through the gasifier ($0.794 \times 10^{-3} \text{ m}^3/\text{s} \cdot \text{kg}$) and there was no air routed to the burner. At the beginning of gasification, the outlet temperature at 450 mm was very low, at room temperature, because the hot flue gas had not had time to have a great influence. With increasing operating time, the high temperature zone moved upwards and the outlet temperature increased to 267 °C after 30 min.

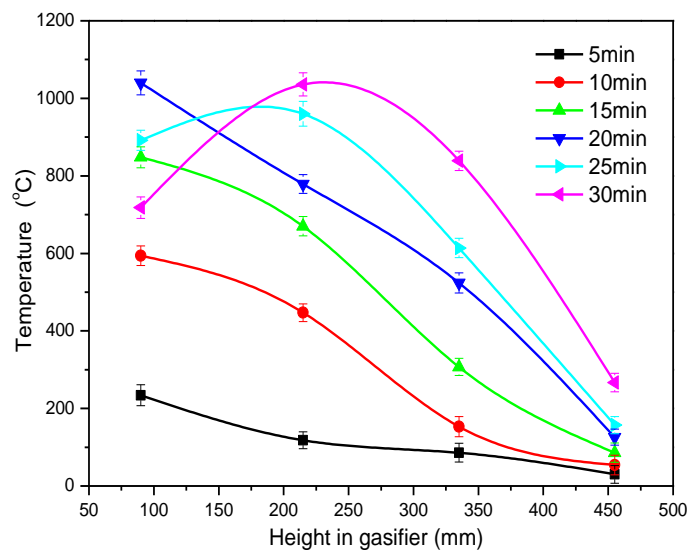


Fig. 3. Temperature distribution in gasifier ($0.794 \times 10^{-3} \text{ m}^3/\text{s} \cdot \text{kg}$)

As shown in Fig. 4, the outlet gas composition stabilized approximately 20 min after ignition.

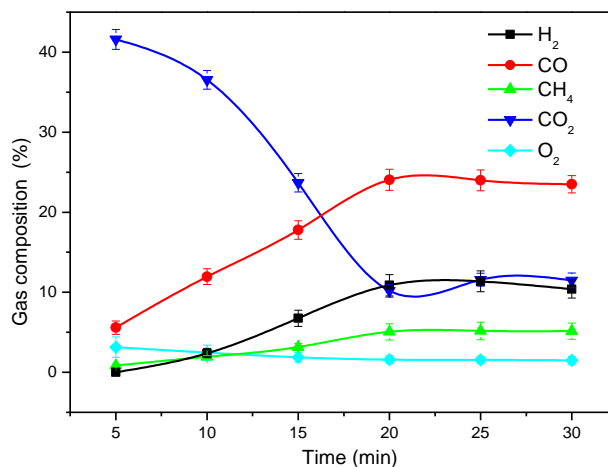


Fig. 4. Outlet gas composition change with time ($0.794 \times 10^{-3} \text{ m}^3/\text{s} \cdot \text{kg}$)

In the first 20 min, the temperature decreased along the gasifier height from the bottom to the top, and the highest temperature was always at the bottom oxidation layer. However, after 20 min, when the gasification stove system reached stable conditions, the highest temperature moved upwards, to about 220 mm. Under stable operation, the highest temperature was mostly in the range of 950 to 1050 °C. Such a layered temperature distribution was useful and can be used for modeling and analysis of the reaction process inside the gasifier.

Gas composition

After ignition, the outlet gas was sampled and analyzed using GC every 5 min; the gas composition over time is shown in Fig. 4. In the first 5 min, the CO₂ content was very high because biomass combustion had begun in the oxygen layer but the reaction in the pyrolysis and reducing layers was slight. With increasing operating time, the content of CO and H₂ increased because the high-temperature zone moved upwards, as shown in Fig. 3. The operating condition tended toward stability; after 20 min, the gas composition remained unchanged. Under stable conditions, CO was most abundant at approximately 25%, the contents of CO₂ and H₂ were approximately 10%, and CH₄ accounted for approximately 4% of the gas produced. There was a small amount of O₂ at the outlet from unreacted air.

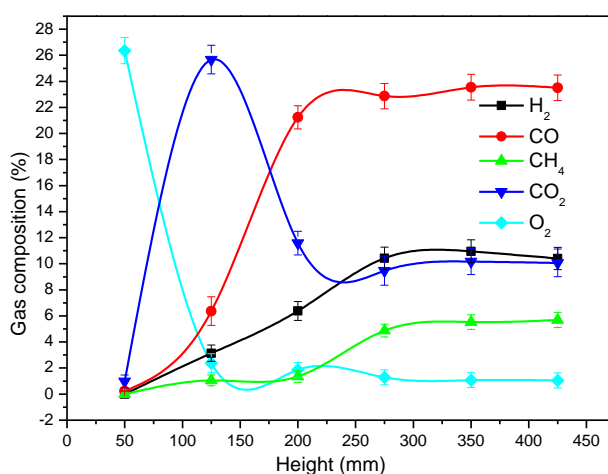


Fig. 5. Gas composition distribution in gasifier ($0.794 \times 10^{-3} \text{ m}^3/\text{s} \cdot \text{kg}$)

Under stable operating conditions, the gas distribution at six positions along the gasifier height was measured, as shown in Fig. 5. The O₂ concentration was notably high at 50 mm, but it dropped to almost zero at 150 mm. This was because the ash zone was below 50 mm and no oxidation reaction occurred in this zone. In the oxidation layer from 50 to 100 mm, O₂ was quickly consumed and the CO₂ content rose rapidly. In this oxidation layer, the CO content rose very slowly because of the excess air used.

In the layer from 125 to 200 mm, the CO₂ content dropped rapidly and the CO content rose rapidly, indicating this was the reducing layer in which CO₂ was reduced to CO by char according to reaction R₄. In this layer, the H₂ content also increased as reactions R₅ and R₆, while the increase in CH₄ content was very slow, indicating that reactions R₇ through R₁₁ occurred at slow rates. In the layer from 200 to 300 mm, the CH₄ and H₂ contents continued to rise, but the CO content was almost stable, indicating that this was the pyrolysis layer and that the hydrocarbons were mostly from the pyrolysis

reaction. In the layer above 300 mm, all gas concentrations were stable, indicating that this was the drying layer, inside of which no remarkable reactions took place.

Effect of Air Quantity into Gasifier

Temperature

In this group of tests, all air passed through the gasifier and there was no air fed to the burner. The effect of the quantity of air into the gasifier on the temperature distribution is shown in Fig. 6. Figure 6(a) shows that changing the air quantity in the range tested did not affect the overall trend of the temperature distribution. However, the data in Fig. 6(b) suggest that the effect of air quantity was greater. With increasing air quantity, the temperatures in the oxidation and reducing layers increased, reaching maxima at $0.794 \times 10^{-3} \text{ m}^3/\text{s}\cdot\text{kg}$. With further increase in the air quantity, the temperatures decreased, meaning that there was an optimum quantity of air to achieve the highest stove temperature and enhance the reactions in the stove.

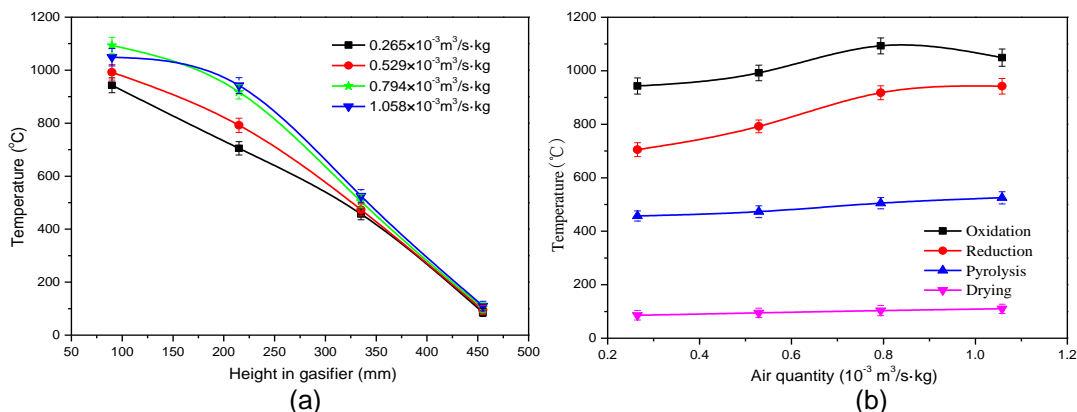


Fig. 6. Effect of air quantity on temperature distributions

Gas composition

The effect of air quantity into the gasifier on gas composition is shown in Fig. 7. Increasing the air quantity increased the H_2 content from 7% to 11% and the O_2 content from 2.12% to 2.96% but decreased the CH_4 content from 9.33% to 6.30%. The changes in CO and CO_2 contents were inversely related.

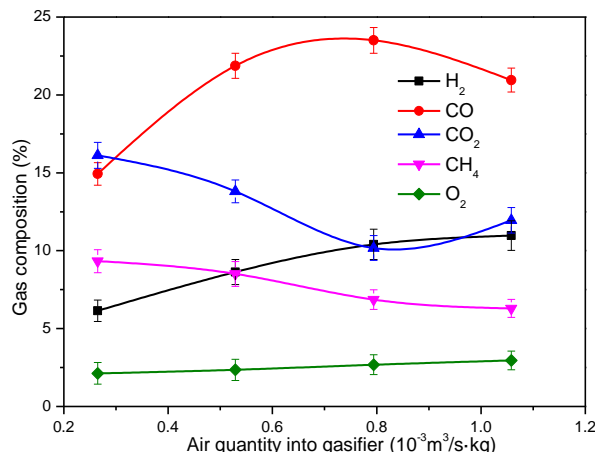


Fig. 7. Effect of air quantity on gas composition

The changed amounts of CO and CO₂ were almost equal, indicating the transformation between CO₂ and CO. Because reaction R₄ was endothermic, the equation R₄ went in the direction of producing CO. So, an increase of air flow rate increases the amount of CO but reduces the amount of CO₂ produced. CO accounted for most of the produced gases, and it was found that the content of CO reached a maximum at $0.794 \times 10^{-3} \text{ m}^3/\text{s} \cdot \text{kg}$, which also yielded the maximum reaction temperature in oxidation and reducing layers. This further demonstrated the existence of an optimum air quantity into the gasifier and that higher reaction temperatures enhanced endothermic reducing reactions such as R₄, R₅, and R₆.

Gasifier and stove performances

The effects of the air quantity into the gasifier on the stove performance are listed in Table 2. With increasing air quantity from 0.265 to 1.058 $\text{m}^3/\text{s} \cdot \text{kg}$, the gas yield increased from 1.43 to 1.59 m^3/kg . The gas heating value reached a maximum at the air quantity of $0.794 \times 10^{-3} \text{ m}^3/\text{s} \cdot \text{kg}$. This was due to the gas composition, as can be seen in Fig. 7. At the optimum air quantity, a large amount of CO₂ was transformed into combustible CO, yielding the highest gasification efficiency of 33.59%. The carbon conversion efficiency reached a maximum of 63.83% at $0.529 \times 10^{-3} \text{ m}^3/\text{s} \cdot \text{kg}$ during the texts examined.

Table 2. Stove Performance with Various Air Quantities Introduced into the Gasifier

-	Name	Condition 1	Condition 2	Condition 3	Condition 4
Air	Air quantity ($10^{-3} \text{ m}^3/\text{s} \cdot \text{kg}$)	0.265	0.529	0.794	1.058
Water	Water Initial Temperature (°C)	11	11	9	10
	Water After Boiling (°C)	99.5	99.8	100.5	100
	Water Initial Mass (kg)	2	2	2	2
	Water Final Mass (kg)	1.896	1.74	1.72	1.761
	Time for Water Boiling Test (s)	2100	960	840	870
Gasifier	Gas Yield (m^3/kg)	1.43	1.47	1.53	1.59
	Gas Heating Value (MJ/m^3)	5.90	6.24	6.48	6.08
	Carbon Conversion Efficiency (%)	61.84	63.81	60.20	57.22
	Gasification Efficiency (%)	31.47	32.82	33.59	31.96
Stove	Stove Power (kW)	0.464	1.385	1.664	1.286
	Stove Thermal Efficiency (%)	22.001	30.015	32.632	31.253

Because there was no air passing through the burner in this group of tests, the gas combustion on the burner should be *via* typical diffusion combustion. Under these conditions, the stove performance should be determined primarily by the performances of the gasifier. Consequently, at the optimum air quantity of $0.794 \times 10^{-3} \text{ m}^3/\text{s} \cdot \text{kg}$, both the output power and the thermal efficiency reached their maximum values, of 1.664 kW and 32.632%, respectively.

Effect of Air Distribution (Air Quantity through Burner) on Stove Efficiency

Air passing through the burner is also very important for stove efficiency. To determine the effect of the air quantity passed through the burner, the air quantity through the gasification stove was kept constant at the optimum value of $0.794 \times 10^{-3} \text{ m}^3/\text{s} \cdot \text{kg}$ and

the air quantity through the burner was varied. The three tested conditions were air ratios of 0.2, 0.333, and 0.428, as shown in Table 3.

Table 3. Stove Performance When Changing the Air Quantity through Burner

-	Name	Condition 4	Condition 5	Condition 6	Condition 7
Air	Ratio of Air Quantity of Burner and Gasifier (1)	0.000	0.200	0.333	0.428
Water	Water Initial Temperature (°C)	9	11	10	10
	Water After Boiling (°C)	100.5	99.5	100	99
	Water Initial Mass (kg)	2	2	2	2
	Water Final Mass (kg)	1.72	1.762	1.76	1.773
	Time for Water Boiling Test (s)	840	750	720	840
Stove	Stove Power (kW)	1.664	1.734	1.798	1.697
	Stove Thermal Efficiency (%)	32.632	34.873	36.527	33.122

The air quantity through the gasifier was constant at $0.794 \times 10^{-3} \text{ m}^3/\text{s} \cdot \text{kg}$.

With increasing air quantity through the burner, the time required to boil the water first decreased and then increased, whereas the stove power and thermal efficiency increased and then decreased. The optimum air distribution was a ratio of 0.333 between the air to the burner and gasifier. Under the optimum conditions, the stove power increased from 1.664 (diffusion flame with no air through the burner) to 1.798 kW (partial premixed flame with optimum air through the burner) and the thermal efficiency increased from 32.632% to 36.527%. The best operating condition for a partial premixed flame yielded an additional 0.134 kW of power and 3.895% thermal efficiency as compared with the diffusion flame.

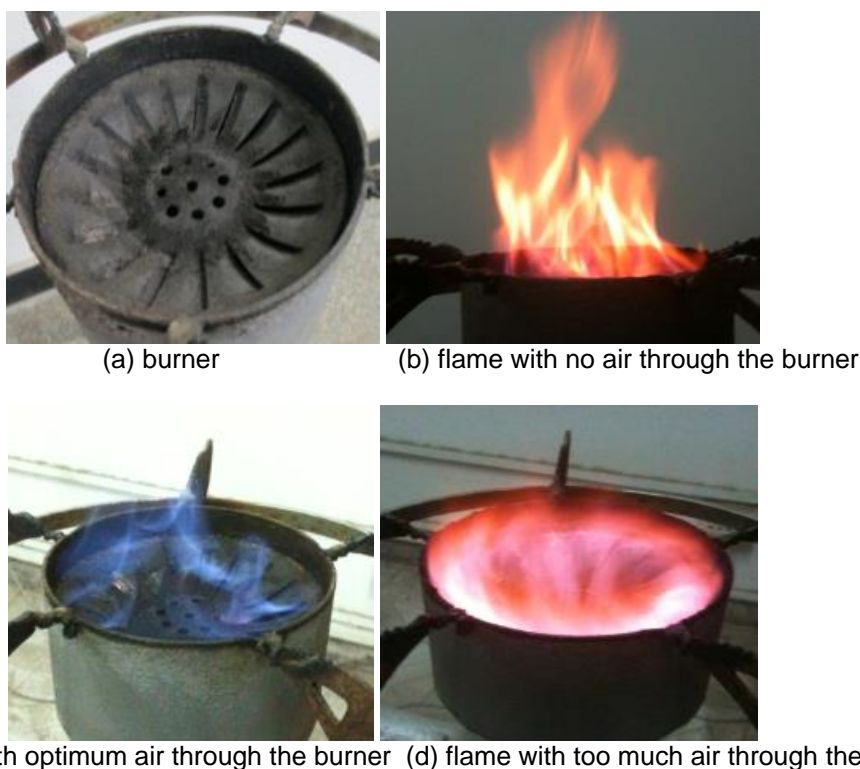


Fig. 8. Flames with various air quantities through the burner

The flame appearance with various burner air quantities is shown in Fig. 8. Three kinds of flames were observed. Figure 8(a) shows the burner employed in this study, in which the gasified gas flowed through the central, circular holes and air passed through the swirling, inclined channels around these holes.

When no air passed through the burner and all the air went directly into the stove, the flame on the burner was a typical diffusion flame, as shown in Fig. 8(b). Under these conditions, there was no air from the swirling channels available to be mixed with the gasified gas from the central holes; consequently, the flame was very long, unstable, and had a yellow-red color.

With increasing air quantity passing through the burner, the flame length was remarkably reduced because the injection of supplementary air from the swirling, inclined channels mixed rapidly with the gasified gas. The flame color gradually changed from yellow-red to blue, as shown in Fig. 8(c). A blue flame produces much higher temperatures than a yellow-red flame and the blue flame exhibits much higher thermal efficiency. This is why, under these conditions, the stove power and efficiency were the highest, as shown in Table 3.

When the burner air was increased even further, the swirling air quantity was excessive and led to a normal flame submerged by such high-speed air coming from the swirling, inclined channels. Moreover, because the tangential momentum of the swirling flow was too large, the energy loss in the tangential direction increased and the flame area touching the bottom of the water pot was reduced. This is why the power and thermal efficiency decreased when burner air was further increased.

CONCLUSIONS

1. The producer gas composition and energy output stabilized 15 min after ignition, and the highest temperature was at the bottom oxidation layer of the gasifier, in the range of 950 to 1050 °C. Along the gasifier height from bottom to top, the contents of H₂, CO, and CH₄ increased until 250 mm and the content of CO₂ reached a peak value at approximately 150 mm.
2. There was an optimum air quantity at approximately $0.794 \times 10^{-3} \text{ m}^3/\text{s} \cdot \text{kg}$ that yielded the best gasifier performance. With increasing air quantity into the gasifier, the stove temperature, contents of CO and H₂ in the producer gas, gas heating value, and gasification efficiency first increased and then decreased. The highest gas heating value and gasification efficiency were 6.48 MJ/m³ and 33.59%, respectively.
3. The best stove performance was obtained at an optimum air distribution ratio of 0.333 between the burner and gasifier air ($0.794 \times 10^{-3} \text{ m}^3/\text{s} \cdot \text{kg}$). Under these conditions, the stove power and thermal efficiency reached 1.798 kW and 36.527%, respectively.
4. With increasing air quantity passing through the burner, the flame length above the burner was remarkably reduced and the flame color gradually changed from yellow-red to blue. At the optimum air distribution ratio of 0.333, the flame color showed blue and stable.

ACKNOWLEDGMENTS

This study was supported by the National Natural Science Foundation of China (Nos. 51306142 and 51376147) and the Fundamental Research Funds for the Central Universities.

REFERENCES CITED

- Bailis, R., Berrueta, V., Chengappa, C., Dutta, K., Edwards, R., Masera, O., and Smith, K. R. (2007). "Performance testing for monitoring improved biomass stove interventions: Experiences of the Household Energy and Health Project," *Energy for Sustainable Development* 11(2), 57-70. DOI: 10.1016/S0973-0826(08)60400-7
- Ballard-Tremere, G., and Jawurek, H. H. (1996). "Comparison of five rural, wood-burning cooking devices: Efficiencies and emissions," *Biomass & Bioenergy* 11(5), 419-430. DOI: 10.1016/S0961-9534(96)00040-2
- Bhattacharya, S. C., and Salam, P. A. (2002). "Low greenhouse gas biomass options for cooking in the developing countries," *Biomass & Bioenergy* 22(4), 305-317. DOI: 10.1016/S0961-9534(02)00008-9
- Boy, E., Bruce, N., Smith, K. R., and Hernandez, R. (2000). "Fuel efficiency of an improved wood-burning stove in rural Guatemala: Implications for health, environment and development," *Energy for Sustainable Development* 4(2), 23-31. DOI: 10.1016/S0973-0826(08)60239-2
- Brauer, M., Bartlett, K., Regalado-Pineda, J., and Perez-Padilla, R. (1995). "Assessment of particulate concentrations from domestic biomass combustion in rural Mexico," *Environmental Science & Technology* 30(1), 104-109. DOI: 10.1021/es9501272
- Ezzati, M., and Kammen, D. M. (2001). "Indoor air pollution from biomass combustion and acute respiratory infections in Kenya: an exposure-response study," *The Lancet* 358(9282), 619-624. DOI: 10.1016/S0140-6736(01)05777-4
- Huangfu, Y., Li, H., Chen, X., Xue, C., Chen, C., and Liu, G. (2014). "Effects of moisture content in fuel on thermal performance and emission of biomass semi-gasified cookstove," *Energy for Sustainable Development* 21, 60-65. DOI: 10.1016/j.esd.2014.05.007
- Jetter, J., Zhao, Y., Smith, K. R., Khan, B., Yelverton, T., DeCarlo, P., and Hays, M. D. (2012). "Pollutant emissions and energy efficiency under controlled conditions for household biomass cookstoves and implications for metrics useful in setting international test standards," *Environmental Science & Technology* 46(19), 10827-10834. DOI: 10.1021/es301693f
- Johnson, M., Lam, N., Brant, S., Gray, C., and Pennise, D. (2011). "Modeling indoor air pollution from cookstove emissions in developing countries using a Monte Carlo single-box," *Atmospheric Environment* 45(19), 3237-3243. DOI: 10.1016/j.atmosenv.2011.03.044
- Koyuncu, T., and Pinar, Y. (2007). "The emissions from a space-heating biomass stove," *Biomass & Bioenergy* 31(1), 73-79. DOI: 10.1016/j.biombioe.2006.06.014
- Li, B., Chen, H., Yang, H., Wang, X., and Zhang, S. (2011). "Development and improvement of household updraft biomass gasifier," *Transactions of the Chinese Society of Agricultural Engineering* 27(S1), 205-209 (in Chinese)

- Li, Y., Wu, J., and Yang, Y. (2011). "Design and performance test of civil biomass stover combined gasifier-burner," *Renewable Energy Resources* 29(6), 153-159 (in Chinese)
- MacCarty, N., Ogle, D., Still, D., Bond, T., and Roden, C. (2008). "A laboratory comparison of the global warming impact of five major types of biomass cooking stoves," *Energy for Sustainable Development* 12(2), 56-65. DOI: 10.1016/S0973-0826(08)60429-9
- McCracken, J. P., and Smith, K. R. (1998). "Emissions and efficiency of improved woodburning cookstoves in Highland Guatemala," *Environment International* 24(7), 739-747. DOI: 10.1016/S0160-4120(98)00062-2
- Panwar, N. L. (2009). "Design and performance evaluation of energy efficient biomass gasifier based cookstove on multi fuels," *Mitigation and Adaptation Strategies for Global Change* 14(7), 627-633. DOI: 10.1007/s11027-009-9187-4
- Panwar, N. L. (2010). "Performance evaluation of developed domestic cook stove with *Jatropha* shell," *Waste and Biomass Valorization* 1(3), 309-314. DOI: 10.1007/s12649-010-9040-8
- Qiu, D., Gu, S., Catania, P., and Huang, K. (1996). "Diffusion of improved biomass stoves in China," *Energy Policy* 24(5), 463-469. DOI: 10.1016/0301-4215(96)00004-3
- Reddy, M. S., and Venkataraman, C. (2002). "Inventory of aerosol and sulphur dioxide emissions from India. Part II—Biomass combustion," *Atmospheric Environment* 36(4), 699-712. DOI: 10.1016/S1352-2310(01)00464-2
- Smith, K. R., Khalil, M. A. K., Rasmussen, R. A., Thorneloe, S. A., Manegdeg, F., and Apte, M. (1993). "Greenhouse gases from biomass and fossil fuel stoves in developing countries: A Manila pilot study," *Chemosphere* 26(1), 479-505. DOI: 10.1016/0045-6535(93)90440-G
- Smith, K. R., Uma, R., Kishore, V. V. N., Zhang, J., Joshi, V., and Khalil, M. A. K. (2000). "Greenhouse implications of household stoves: An analysis for India," *Annual Review of Energy and the Environment* 25(1), 741-763. DOI: 10.1146/annurev.energy.25.1.741
- Wang, X., Hu, Z., Deng, S., Wang, Y., Wei, B., and Tan, H. (2014). "Investigation on the synergetic effect of biomass co-firing in the atmosphere of O₂/CO₂," *Journal of Biobased Materials and Bioenergy* 8(5), 481-488.
- Wang, X., Si, J., Tan, H., Niu, Y., Xu, C., and Xu, T. (2012). "Kinetics investigation on the combustion of waste capsicum stalks in Western China using thermogravimetric analysis," *Journal of Thermal Analysis and Calorimetry* 109(1), 403-412.
- Yuntenwi, E. A., MacCarty, N., Still, D., and Ertel, J. (2008). "Laboratory study of the effects of moisture content on heat transfer and combustion efficiency of three biomass cook stoves," *Energy for Sustainable Development* 12(2), 66-77. DOI:10.1016/S0973-0826(08)60430-5

Article submitted: February 6, 2015; Peer review completed: April 26, 2015; Revisions received and accepted: May 18, 2015; Published: May 22, 2015.

DOI: 10.15376/biores.10.3.4178-4190